Universiteit Utrecht

D^{*+} nuclear modification factor versus centrality in lead-lead collisions at $\sqrt{s_{NN}}$ = 2.76 TeV at ALICE

-

Sjoerd Cornelissen

February 19, 2013

Bachelor Thesis
Report number: UU(SAP) 13-3

Supervisors:
Dr. André Mischke
Dr. Alessandro Grelli

Utrecht University
Faculty of Science/Department of Physics and Astronomy
Institute for Subatomic Physics
Buys Ballot laboratory
PO BOX 80 000, 3508 TA Utrecht, The Netherlands

D^{*+} nuclear modification factor versus centrality in lead-lead collisions at $\sqrt{s_{NN}} = 2.76\,\mathrm{TeV}$ at ALICE

Sjoerd Cornelissen
Utrecht University

February 19, 2013

Abstract

From Quantum Chromodynamics it follows that at extremely high energies, quarks and gluons can be found in a deconfined state, called the Quark-Gluon Plasma (QGP). The ALICE detector at CERN was built to study lead-lead collisions at energies high enough to produce the QGP. In this thesis we study the production of D^{*+} mesons versus centrality in lead-lead collisions at $\sqrt{s_{NN}}$ = 2.76 TeV with the ALICE experiment at the Large Hadron Collider at CERN. With this study we will calculate the systematic uncertainty of the measurement. Also, we will determine the reconstruction efficiency of the detector. Then we can calculate the Nuclear Modification Factor R_{AA}, which is the ratio of produced D mesons in Pb-Pb collisions compared to p-p collisions. Because particles lose energy in the dense QGP, we will measure less D mesons at high p_{T} in Pb-Pb collisions. The actual R_{AA} enables us to test the models which are used to predict the properties of the QGP.

Three detectors of the ALICE experiment are used for this study: the Inner Tracking System (ITS), the Time Projection Chamber (TPC) and the Time of Flight detector (TOF). We need those to reconstruct the D^{*+} and the D^0 daughter from the measured particles. We then determined the raw yield in 2 p_{T} ranges and 5 centrality bins. To determine the systematic uncertainty, we analyzed the stability of the yield when using different fitting functions and ranges, and also bin counting. The systematic error of the yield was approximately 3-6%, but varied with the centrality and p_{T}. The efficiency turned out to be approximately 10%. Then calculating the R_{AA}, we found it was approximately 0.2 for the most central collisions and was closer to unity for the more peripheral collisions.

Contents

1 Introduction

1.1 Theoretical background

Quantum Chromodynamics (QCD) is the theory concerned with strong interaction, one of the four fundamental interactions of physics (the others being the weak interaction, gravitation and electromagnetic interaction). QCD is part of the Standard Model of particle physics. It combines three of the four known forces (weak, strong and electromagnetic force). QCD describes interactions between quarks and gluons. Normally, QCD predicts that quarks are confined, requiring an infinite amount of energy to separate quarks from each other. This is also why no isolated quark has ever been observed. At the same time, QCD also predicts that at extremely high energy densities, matter will enter a new state, known as the Quark-Gluon Plasma (QGP). In this state, gluons and quarks are actually deconfined and can be seen separately from each other (see Figure 1).

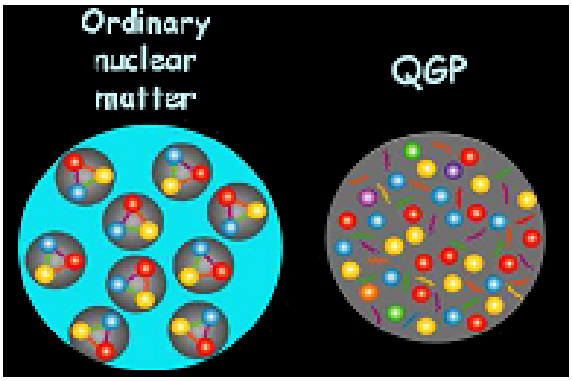

Figure 1: A schematic representation of the QGP (right) compared to hadronic matter (left) [1].

The world's largest high energy particle accelerator, the Large Hadron Collider (LHC), at the European Organization for Nuclear Research (CERN), has the ability to provide lead-lead collisions at an energy high enough to create a QGP. This study uses collisions with an energy of $\sqrt{s_{NN}} = 2.76$ TeV per nucleon nucleon pair. The detector dedicated to heavy ion physics at the LHC is called ALICE (A Large Ion Collider Experiment). It is a multi purpose detector built to study the QGP properties via the study of light quarks, heavy quarks and jets.

We can infer the properties of the QGP by comparing the proton-proton and lead-lead collisions. One might expect that Pb-Pb collisions are just a superposition of 208 p-p collisions, since there are 208 nucleons in a lead nucleus. We should, by this argumentation, detect 208 times the number of partons. This turns out not to be the case. First of all, we have to correct for the fact that in Pb-Pb collisions, the number of actual nucleons colliding is not 208. But there is another reason we do not find that number of particles. In the proton-proton collisions, the energy density is not high enough to produce a QGP, whereas in the lead-lead collisions it is. The quarks that are created in the collisions will lose energy in the dense QGP that is created. This will result

in a different kinematic of the hadron created during the quarks hadronization phase. Therefore, we should in fact expect to find less hadrons at the higher energy levels compared to the ones found in the corresponding p-p collisions. The fraction of D^{*+} mesons that is created in lead-lead collisions compared to proton-proton collisions is called the nuclear modification factor R_{AA}^{D}, which is defined as

$$R_{\mathrm{AA}} = \frac{1}{\langle N_{\mathrm{binary}} \rangle} \frac{\mathrm{d}^2 N_{\mathrm{PbPb}} / \, \mathrm{d}p_{\mathrm{T}} \, \mathrm{d}y}{\mathrm{d}^2 N_{\mathrm{pp}} / \, \mathrm{d}p_{\mathrm{T}} \, \mathrm{d}y} \tag{1}$$

Here $\langle N_{\mathrm{binary}} \rangle$ is the average number of binary collisions in a lead-lead collision, $\mathrm{d}N_{\mathrm{PbPb}} / \, \mathrm{d}p_{\mathrm{T}}$ the lead-lead p_{T} spectrum and $\mathrm{d}N_{\mathrm{pp}} / \, \mathrm{d}p_{\mathrm{T}}$ the proton-proton p_{T} spectrum. From this equation, it follows directly that it is important to have a good knowledge of the proton-proton collisions. A lot of information can be found in [2] and [3]. The nuclear modification factor will have a value of 1 in the absence of a QGP, and a value $R_{\mathrm{AA}} < 1$ when there is a QGP present. Consequently, it is a very important number, since it enables to study the properties (including the density) of the QGP.

1.2 Motivation and outline

In this thesis, we will investigate the properties to the nuclear modification factor versus the event centrality. The data consists of Pb-Pb collisions from 2011 with a center of mass energy of 2.76 TeV. The centrality is a gauge for the amount of overlap particles have at the moment of the collision. For a perfect head-on collision, associated with a centrality of 0%, we have a superposition of the nuclei. When we go to more peripheral collisions, with higher centralities, the superimposition is less and less. If the collision is very central, more energy is associated with it than if it is a more peripheral one. Therefore, the created QGP is denser and larger. Hence, the (charm) quarks that are produced in the central collisions lose more energy than the ones produced in the peripheral collisions, inter alia due to more collision with gluons and quarks in the QGP (see Figure 2). We therefore expect that the nuclear modification factor for the higher centralities is closer to 1. From this study we can determine the effects the centrality has on the created QGP.

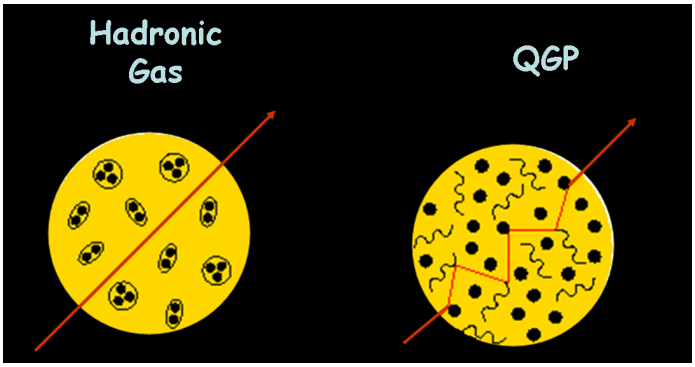

Figure 2: A quark passes through hadronic matter undisturbed (left), while it loses energy due to collisions with quarks and gluons in the QGP (right) [1].

Firstly, we will have a look into the methods used to determine the yield. We need to have an idea of what detectors are being used at CERN for this study. Then, we will study what needs to be done to reconstruct the D mesons from the data. Since we are interested in the decay $D^{*+} \rightarrow D^0 \pi_s^+$, which is a strong decay and thus happens almost instantly, we cannot detect the D mesons itself, but we can measure its decay products, which consist of two pions and a kaon, since the D^0 decays to $D^0 \rightarrow K^- \pi^+$. Once we have reconstructed the topology of the decay, we apply topological selections and particle identification to reduce the combinatorial background. Finally we perform an invariant mass analysis to extract the D^{*+} raw yield. After we have discussed that, we will determine the systematic error on the yield, and the systematic error due to the cuts on the Particle Identification (PID). We get these by determining the stability of the yield: if we compare the yields we get with different fitting functions and ranges, this gives us an idea of the maximum systematic error. Then we need to calculate the efficiency: how many of the original D mesons do we actually measure? Having done that, we come to the final part of this thesis: actually calculating the efficiency and the nuclear modification factor R_{AA}.

2 The ALICE detector

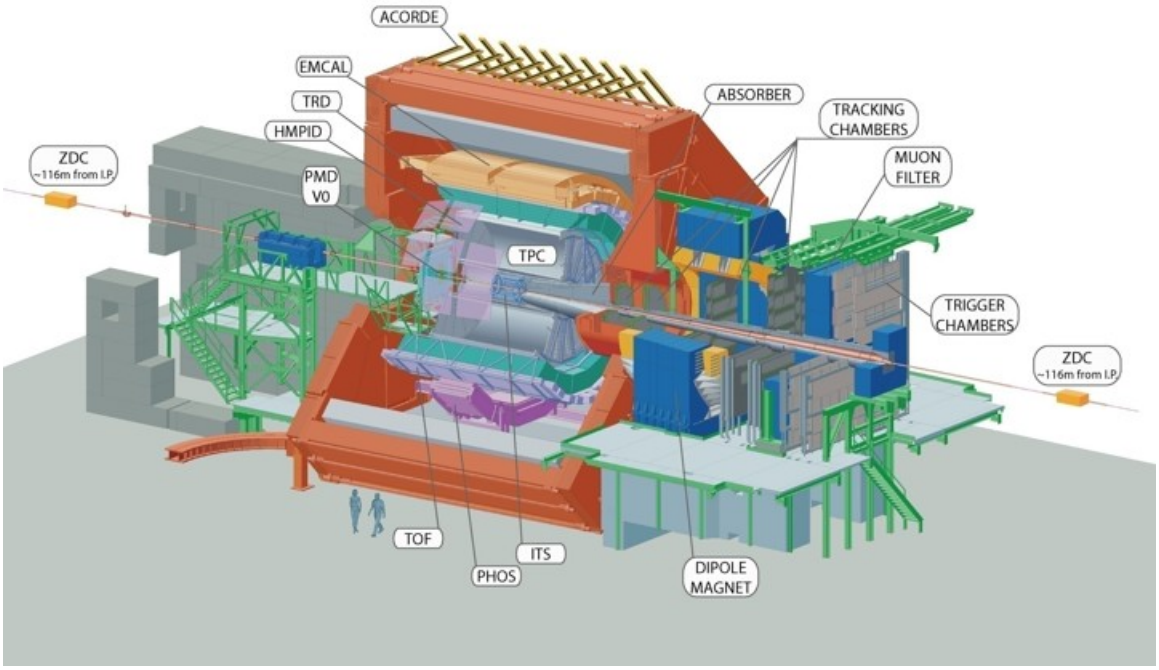

Figure 3: A schematic representation of the ALICE detector [4].

A Large Ion Collider Experiment (ALICE) is one of the four main detectors at LHC. It is a 26 m long, 16 m wide and 16 m high detector consisting of two parts: a forward muon arm and a central barrel.

To indicate the detector acceptance, we can define the pseudorapidity η:

$$\eta = \frac{1}{2} \log \left(\frac{|p| + p_z}{|p| - p_z} \right) \tag{2}$$

A value of $\eta = 0$ corresponds to perpendicular to the beam axis, while a value of $\eta = \infty$ corresponds to parallel to the beam axis.

A closely related variable is the rapidity y:

$$y = \frac{1}{2} \log \left(\frac{E + p_z}{E - p_z} \right) \tag{3}$$

Another variable we will use is the angle of the momentum between the z-axis:

$$\varphi = \text{atan2}\,(-p_y, -p_x) \tag{4}$$

The forward part consists of a muon spectrometer ($-4.0 < \eta < -2.4$), a PMD (Photon Multiplicity Detector, a detector for counting photons), FMD

(Forward Multiplicity Detector, used to determine the multiplicity, has a range up to $\eta = 5.1$), ZDC (Zero Degree Calorimeter, a calorimeter about 90 m away from the primary vertex) and two detectors used for triggering: T0 and V0. The T0 marks the starting time for the TOF which will be explained in more detail below. The V0 triggers all other detectors when it detects a particle.

The central barrel has an acceptance range of $-0.9 < \eta < 0.9$ and consists of (from inside out): the ITS (Inner Tracking System, see section 2.1), TPC (Time Projection Chamber, see section 2.2), TRD (Transition Radiation Detector, used for electron identification), TOF (Time Of Flight, see section 2.3), HMPID (High Momentum Particle Identification Detector) and PHOS (Photon Spectrometer, an electromagnetic calorimeter). The central barrel is installed inside a solenoidal magnet which can generate a magnetic field of up to 0.5 T.

The ITS, TPC and TOF are the most important detectors for our analysis, and will be explained in more depth below.

2.1 Inner Tracking System

Figure 4 shows the layout of the Inner Tracking System (ITS). The ITS is the central-most part of the ALICE detector. It consists of six cylindrical layers of silicon detectors. The first two layers, located at 3.9 cm and 7.6 cm, are made of Silicon Pixel Detectors (SPD). The distance between the beam pipe and the first layer is 0.9 cm. The next two layers are made of Silicon Drift Detectors (SDD) and are located at radii of 15 cm and 23.9 cm. The two outer layers are located at 38.0 cm and 43.0 cm and are made of Silicon Strip Detectors. It is worth mentioning that the Silicon Strip Detectors were built at Utrecht University and NIKHEF Amsterdam.

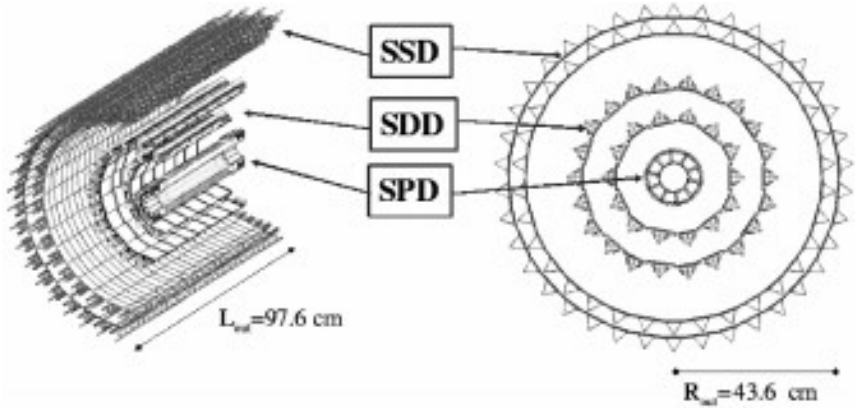

Figure 4: Layout of the Inner Tracking System [4].

The primary use of the ITS is identifying the primary and secondary vertex. As we shall see in section 3.4 vertexing is very important to reconstruct a D^{*+} meson. Since the ITS is crucial for vertexing, we conclude it is very important for this study. It is also used to detect low momentum particles and improve the momentum resolution in general.

Because the first two layers are the closest to the interaction point, the

particle density will be higher compared to the other layers (up to 80 particles per cm^2 in the SPD and < 1 particle per cm^2 in the SSD). This is why the first two layers are made of pixel detectors. These have the largest spatial precision in $r\varphi$: $12\,\mu$m compared to $38\,\mu$m and $20\,\mu$m in the SDD and SSD respectively. The spatial precision in the z direction is $100\,\mu$m for the SPD, $28\,\mu$m for the SDD and $830\,\mu$m for the SSD. The outer layers can have a lower resolution because the particle density will be much less lower.

The outer two layers are also used for connecting the ITS tracks to the TPC tracks and energy deposition measurements ($\mathrm{d}E/\mathrm{d}x$).

2.2 Time Projection Chamber

The Time Projection Chamber (TPC) is the main tracking device in the ALICE detector. Figure 5 shows the layout of the TPC. It is a 510 cm long gas chamber. The gases get ionized when a charged particle passes through, allowing tracking of the particle. The main uses for the TPC are: momentum measurements with a good track separation, track matching with the ITS and TOF and the specific ionisation energy loss ($\mathrm{d}E/\mathrm{d}x$) measurements, which will turn out to be an important player in this thesis.

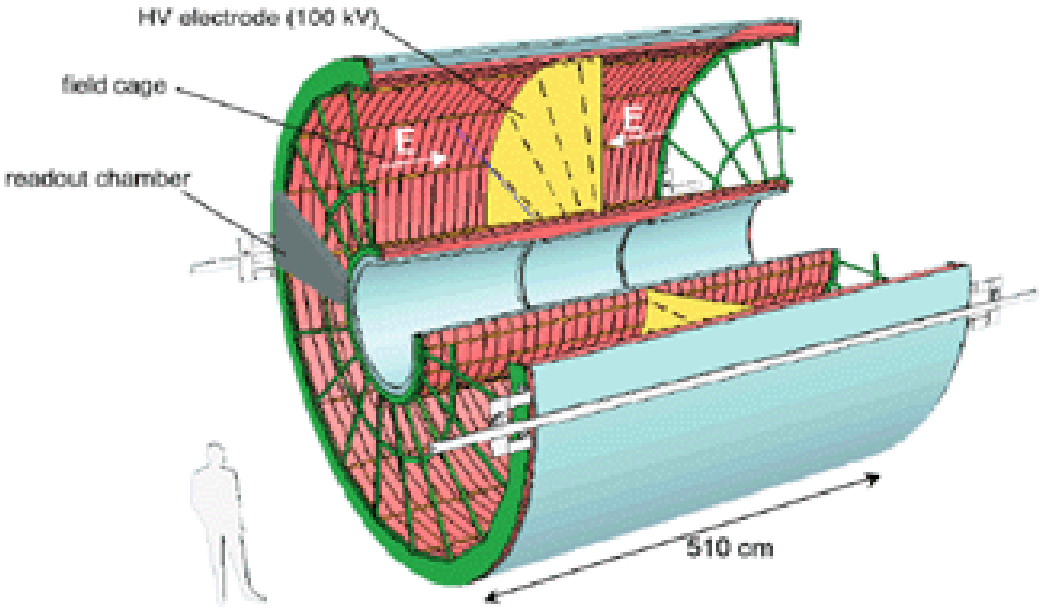

Figure 5: Layout of the Time Projection Chamber [4].

The energy loss measurements are one of the main tools used for particle identification (PID). Different types of particles (p, K, π) have a different energy loss as a function of their momentum. This can be seen in figure 6. By parametrizing these distributions, one can say that with a certain probability (1, 2 or 3σ) the particle has been identified as a proton, kaon or pion. This

procedure is called particle identification.

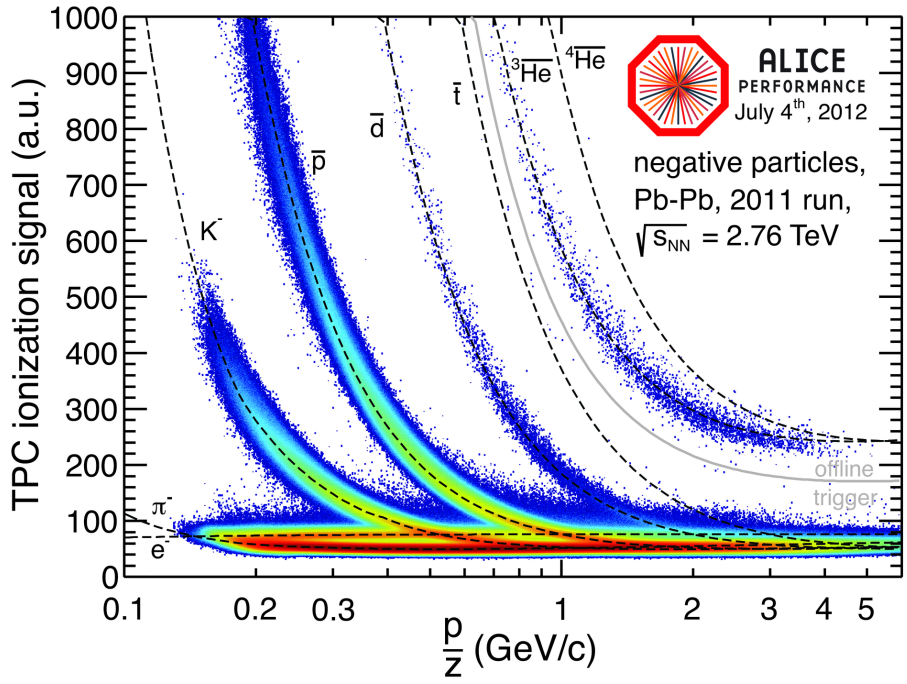

Figure 6: $\mathrm{d}E/\mathrm{d}x$ distribution in the TPC for Pb-Pb collisions at $\sqrt{s_{NN}} = 2.76$ TeV. This can be used for particle identification.

2.3 Time Of Flight

The Time Of Flight detector is designed to measure the flight time a particle passes through it. The TOF alone has a time resolution which is better than 100 ps. It is triggered by the T0, which marks the starting time. Together with the T0 the total timing resolution becomes 160 ps.

The TOF will also be used for particle identification. Heavier particles will travel for a longer time before reaching the TOF, allowing distinction between different particles. Figure 7 shows the velocity versus the momentum/charge. This can be parametrized again, allowing identification of particles with a certain probability.

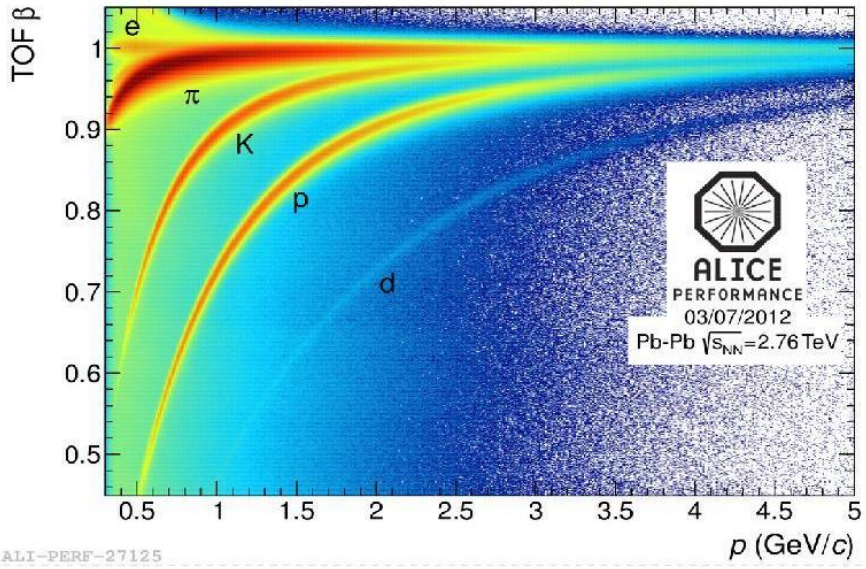

Figure 7: Velocity versus momentum/charge in the TOF detector for Pb-Pb collisions at $\sqrt{s_{NN}} = 2.76$ TeV. This will be used as the TOF PID.

3 D^{*+} meson reconstruction

For this analysis we use the hadronic decay channel, because (semi-)leptonic decay also produces neutrinos, which can not be measured. The decay we are reconstructing is the following. First we use $D^{*+} \rightarrow D^0 \pi_s^+$. The pion which is created here is called the soft pion, because of its low momentum. This decay has a branching ratio of (67.7± 0.5)% [5]. The uncharged D^0 can not be directly detected at ALICE, but since it has a mean lifetime of $(4.101 \pm 0.015) \times 10^{-13}$ s, resulting in a $c\tau$ of about 123 micrometers, its decay secondary vertex is displaced from the primary vertex and can be measured by the detector. The D^0 decay that is used is $D^0 \rightarrow K^- \pi^+$, which has a branching ratio of (3.87 ± 0.05)% [5]. By reconstructing this secondary vertex we resolve the topology of the D^0 decay. It allow us to use topological selections to suppress the combinatoric background. Once the D^0 candidate is reconstructed, we attach to it the pion to get the D^{*+} meson. The reconstruction steps are explained in detail in the following sections.

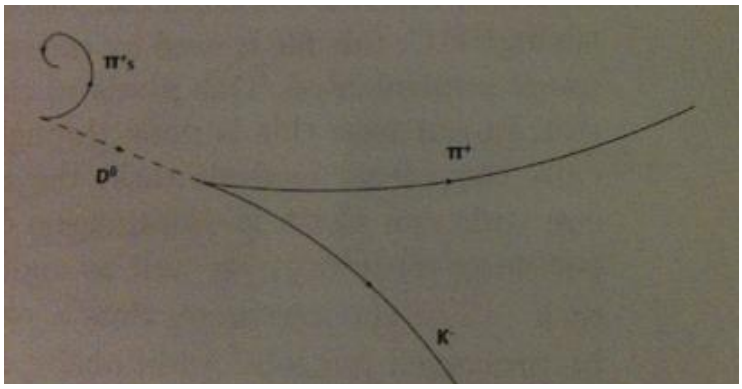

Figure 8: A schematic picture of the decay of the D^{*+} in two steps.

3.1 Reconstruction

In order to reconstruct the D^{*+}, the D^0 has to be reconstructed first. First all negative and positive tracks are combined to form the D^0 candidates. For these candidates the invariant mass is calculated:

$$M(K\pi) = \sqrt{(E_K + E_\pi)^2 - (p_K + p_\pi)^2}. \quad (5)$$

Here p_K is the measured 3-momentum of the negative track, and p_π the measured 3-momentum of the positive track. The variables E_K and E_π are the energies of the particles:

$$E_i^2 = p_i^2 + m_i^2 \quad (6)$$

with m_K and m_π the PDG values of the masses of the kaon and pion.

By doing this we combine the K^- and π^+ from the D^0 decay, but we also combine a lot of tracks that are not from this decay. This results in a large combinatorial background of uncorrelated pairs. In order to reduce this

background, we can apply certain cuts on the tracks, which we will discuss in section 3.4.

To find the D^{*+}, we combine the D^0 candidates with the remaining positive tracks. For this combination we can again calculate the invariant mass:

$$M(K\pi\pi) = \sqrt{(E_K + E_\pi + E_{\pi_s})^2 - (p_K + p_\pi + p_{\pi_s})^2} \tag{7}$$

In this equation p_{π_s} is the measured 3-momentum of the other positive track, and E_{π_s} as defined in (6). As before, we only select the combinations that lie within a range of the D^{*+} mass.

Finally, we search the D^{*+} signal in the mass difference ΔM, which is defined as

$$\Delta M = M(K\pi\pi) - M(K\pi). \tag{8}$$

We expect a sharp peak at about 145.42 MeV/c^2, few MeV above the pion mass. The peak is expected narrow because in the mass difference the resolution effect due to the D^0 cancels out and what contributes to the width of the peak is only the p_T resolution of the soft pion.

3.2 Data and software analysis framework

The data used for this analysis was taken at the LHC run in 2011. The lead-lead collisions had an energy of $\sqrt{s_{NN}} = 2.76$ TeV. Roughly 16 million events in 0-10% centrality and 4 millions in each of the other centrality bins were recorded. To calculate the efficiencies we use a Monte Carlo sample (LHC12a17) based on HIJING event generator. HIJING simulates realistic Pb-Pb collisions. Since we can expect only 1 $c\bar{c}$ pair every 10 events and due to the low reconstruction efficiency of the D^{*+}, it would require a very large amount of HIJING events to have a consistent D^{*+} sample. This generation would result in a large consumption of time and disk space. To avoid this, the HIJING sample was enriched by folding in D^{*+} mesons generated by PYTHIA. The software framework used for the analysis is the official ALICE software, named AliRoot. It is based on ROOT and written in C++. The realistic simulation of the ALICE detector is performed using Geant3.

3.3 Track quality cuts

In order to be sure we only select good tracks, we apply some single track quality selections. The K^- and π^+ are required to have

- ITS refit
- TPC refit and a minimum of 70 (out of a maximum of 159) clusters in TPC
- At least one hit in the SPD
- Minimum p_T of 300 MeV/c for the daughters of the D^0

Refit means that when a track is fitted from the TPC to the ITS, the reverse process after it gives the same track. This will give a greater probability that we have a good track.

The π_s^+ is required to have

- At least one hit in the SPD
- Minimum p_T of 60 MeV/c

3.4 D^{*+} selection cuts

In order to reduce the combinatorial background, cuts are applied on the decay topology of the D^0. In total, 16 cuts are applied. We will review the most important ones.

Because the D^{*+} decays through a strong process, the decay length will be very short. It is below our detector resolution, meaning we do not see the D^{*+} flight line and the decay of the D^{*+} is at the primary vertex. However, the D^0 flies away from the primary vertex a few hundreds of micrometers (having a $c\tau$ of approximately 123 μm), allowing the reconstruction of its flight line. In figure 9 a sketch of the $D^0 \to K^- \pi^+$ decay is shown. The secondary vertex is the point where the D^0 decays.

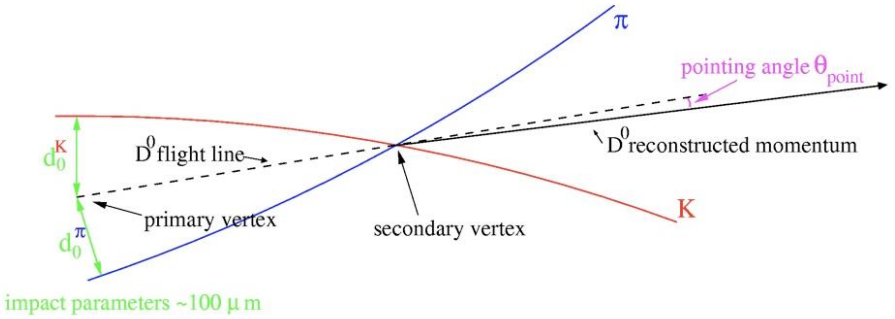

Figure 9: The topology of the $D^0 \to K^- \pi^+$ decay.

When we extrapolate the kaon and pion tracks back, we can define the impact parameter as the distance of closest approach between the track trajectory and the primary vertex. The impact parameter for the kaon is d_0^K and for the pion is d_0^π. It is possible to cut on the impact parameters themselves as well as their product, $d_0^K \times d_0^\pi$. Since the background is completely random, the distribution of the product will be symmetric. As we can see from figure 10 below, the distribution of the signal clearly is not.

The minimum distance between the kaon and pion track is called *dca* (distance of closest approach), which we can cut on. The results for signal can be found in figure 11.

A cut can be made on the cosine of the pointing angle $\theta_{pointing}$. This is the angle between the line from the primary vertex to the secondary vertex (the flight line) and the reconstructed D^0 momentum. The results for signal are shown in figure 12.

A cut is also placed on the momenta of the kaon and pion, p_T^K and p_T^π.

We also cut on the cosine of the angle between the flight line and the kaon momentum in the D^0 rest frame, $\cos\theta^*$.

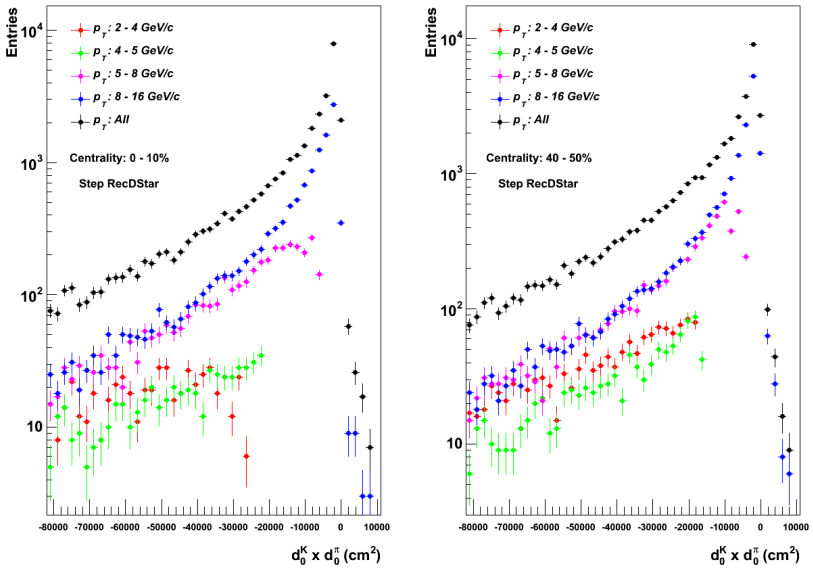

Figure 10: The distribution of the $d_0^K \times d_0^\pi$ for signal for different p_{T}-bins for the most central (left) and most peripheral collisions (right).

In addition to these topological cuts, there is a separate cut, the PID cut. A $n\sigma$ PID means that only particles that have been identified with at least a probability of $n\sigma$ are allowed. The standard PID cuts are 3σ TPC and 3σ TOF PID. We will see in section 5.2 that we have to pay special attention to the careful use of this PID.

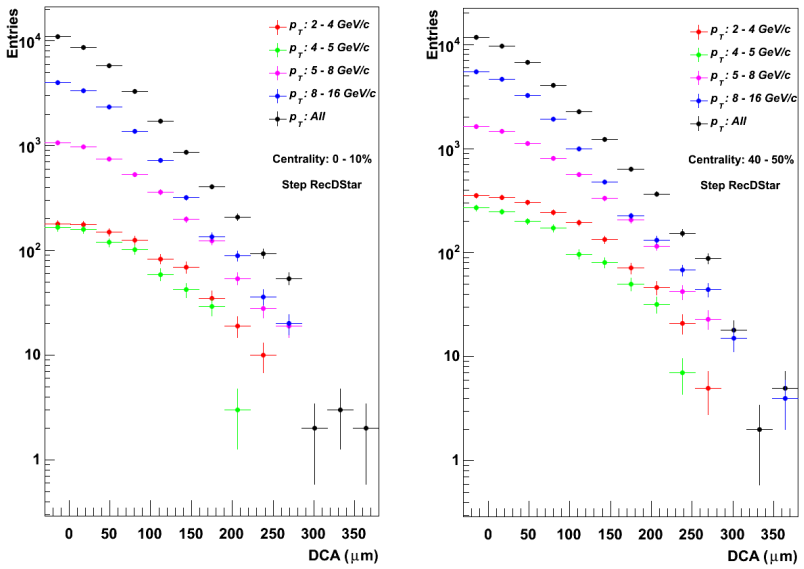

Figure 11: The distribution of the dca for signal for different p_{T}-bins for the most central (left) and most peripheral collisions (right).

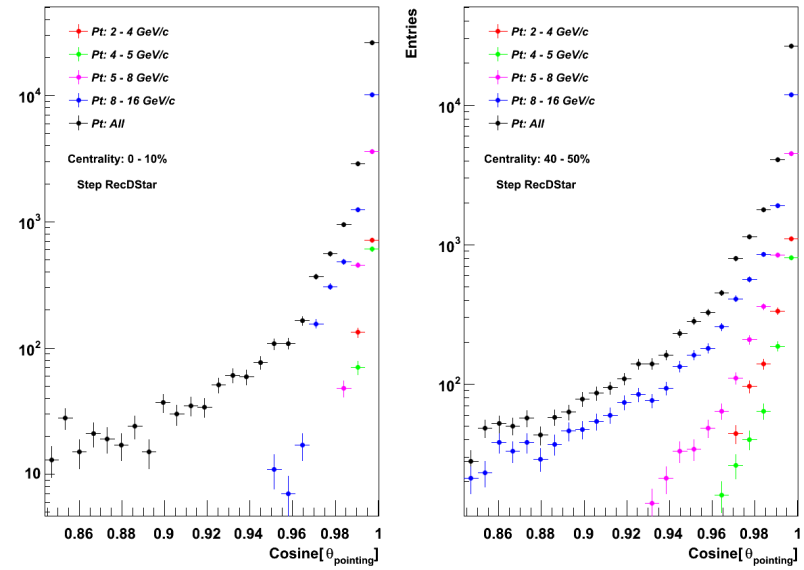

Figure 12: The distribution of the cosine of the pointing angle for signal for different p_{T}-bins for the most central (left) and most peripheral collisions (right).

4 D*+ yield extraction

4.1 Invariant mass analysis

As we mentioned before, we look at the difference of mass between the D^{*+} and D^0, ΔM. Unfortunately, by doing this we find not only the real D^{*+}, but also background of uncorrelated track triplets. We expect the histogram of ΔM to begin at the mass of the pion, and peak at the mass difference between the D^{*+} and the D^0. In figure 13 this is plotted for the measured data, with 2σ TPC and 3σ TOF PID, for p_T between 6 and 12 GeV/c, and centrality between 30 and 40%.

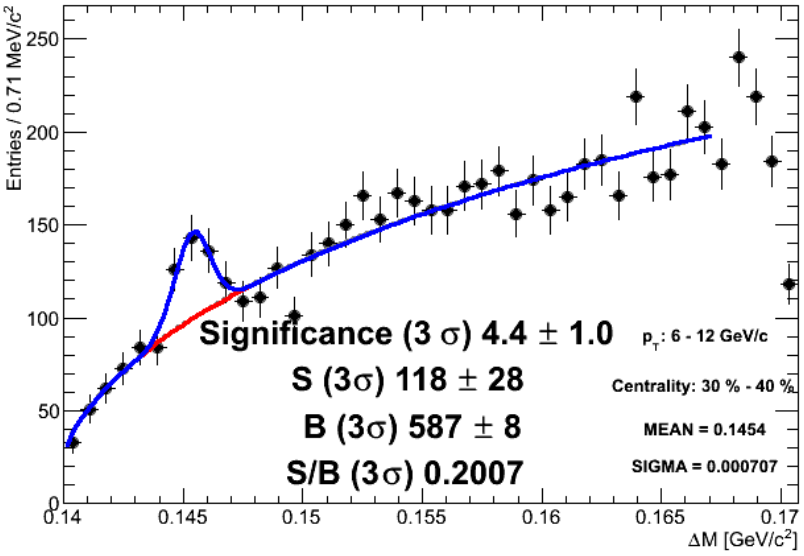

Figure 13: ΔM for 16 million Pb-Pb collisions, for p_T between 6 and 12 GeV/c, and centrality between 30 and 40%. The red line is the fitted background function. The blue full line is the fitted background and signal function.

In this figure we clearly see a combinatorial background and on top of that a peak. The particles that reside under the peak are the real D^{*+}. The area under the peak within 3σ of the peak position is the raw yield. We fit the following function to the histogram:

$$f_{fit}(x) = f_{bkg}(x) + f_{peak}(x) \tag{9}$$

with the background function

$$f_{bkg}(x) = p_0(x - m_\pi)^{\frac{1}{2}}\, e^{p_1(x-m_\pi)} \tag{10}$$

and the Gaussian peak

$$f_{peak}(x) = \frac{p_4}{\sqrt{2\pi p_3^2}} e^{-\frac{(x-p_2)^2}{2p_3^2}} \tag{11}$$

In these equations p_0, p_1, p_2 (position), p_3 (width) and p_4 (yield) are the different fit parameters and m_π is the mass of the pion. The function is fitted in the region $[0.14, 0.167]\,\mathrm{GeV}/c^2$.
The fitting procedure is as follows:

1. Fit f_{fit} to obtain the peak position and the peak width
2. Fit background function f_{bkg} with an excluded region of 3σ around the peak to obtain p_0 and p_1
3. Fit the peak function f_{peak} with fixed background parameters from the previous fit

In this study, the analysis will be done for p_T in the range 6-12 GeV/c and 8-16 GeV/c. This is useful, because this is in the same region other studies have been done, so they can easily be compared. The event centrality was 0-50%, and divided in bins with a width of 10%. In figure 14 the invariant mass and the fits have been plotted for the two different p_T bins and the 5 centrality bins, using a TOF PID of 3σ and a TPC PID of 2σ for centrality between 0 and 20%, and 3σ for higher centralities.

It is important to know how significant our signal is. The quantity to determine whether we have a meaningful result is the significance:

$$\text{Significance } = \frac{S}{\sqrt{S+B}}. \tag{12}$$

In this formula, S is the signal, the number of entries in the gaussian peak within 3σ from the mean. The signal is also known as the yield. B stands for background, the number of entries under the background curve, in the range of 3σ from the mean. A higher significance means we have a clearer signal and our result is also more significant. In scientific papers, results with a significance over 3 are used. The fits used in figure 14 were selected for optimal significance. These ranges are now used for the rest of the analysis.

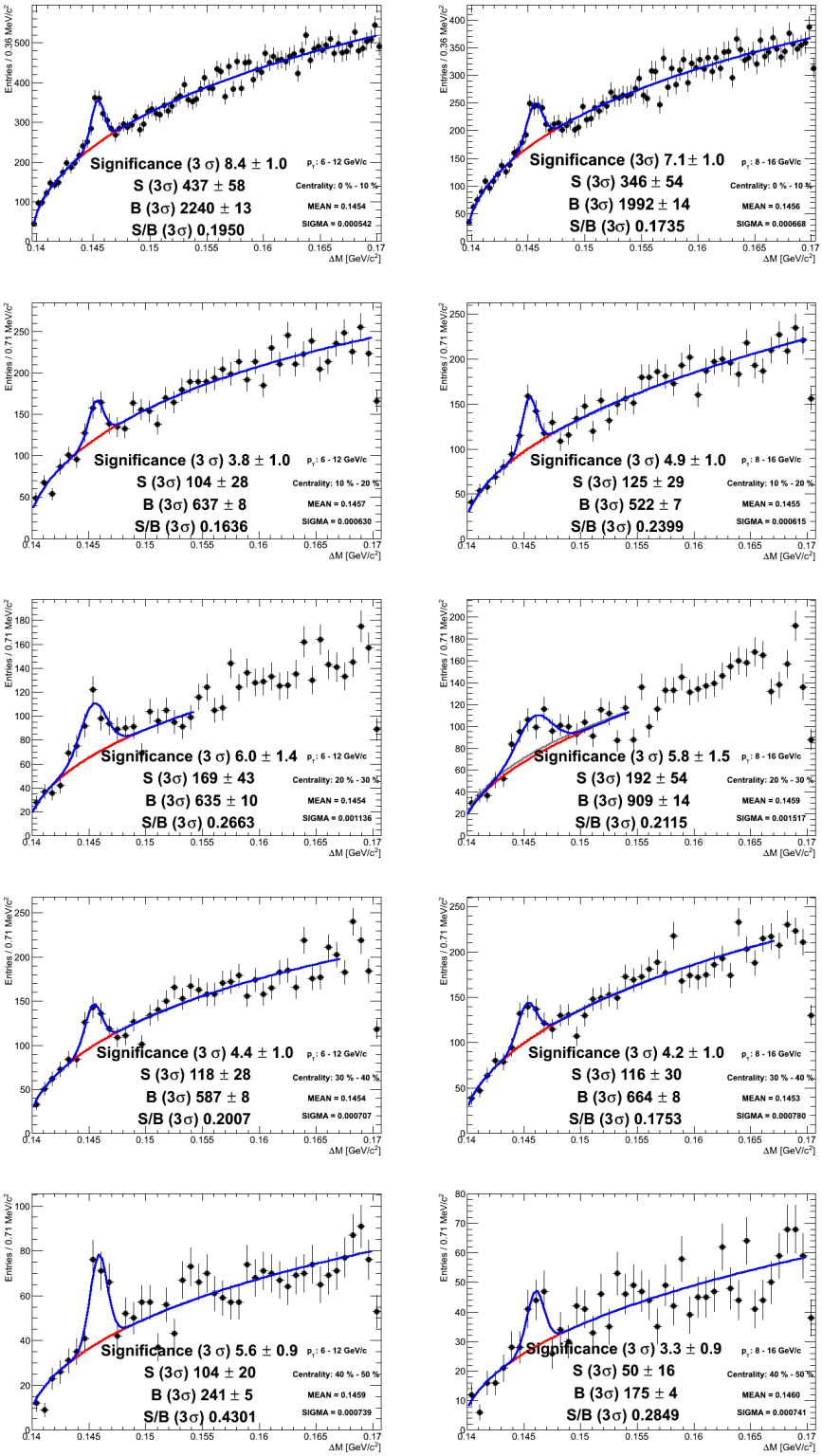

Figure 14: Invariant mass plots for the five centrality bins from top to bottom and the two p_{T} bins from left to right.

5 Systematic errors

5.1 Stability of the yield

Different fitting parameters lead to different yields. If we then look at the ratio of the acquired yield, this gives us an idea of the systematic error of the yield. We define the ratio as

$$\text{Ratio} = \frac{\text{Yield from alternative fit}}{\text{Yield from standard fit}}. \tag{13}$$

Alternative fits may have a different fit range. Our standard fit is in the range $\Delta M = [0.14,0.154]$ MeV/c^2. We can also fit in the range [0.14,0.16] MeV/c^2 and [0.14,0.17] MeV/c^2.

We can also alter the background function used. In our standard fit we use equation 10 to calculate the background. Another possible background function is

$$f_{bkg2}(x) = p_0(x - m_\pi)^{p_1}. \tag{14}$$

In this function, we have dropped the exponential, and the used power is a parameter determined from the fit. Of course, we can also include fits with alterations in both fitting range and background function.

There is one more method of extracting the yield. Instead of using the fit, we can also count the number of entries per bin within 3σ of the peak. If we subtract the background from this, we will get another yield. This method is called bin counting. So for both p_T bins, we have 7 ways of determining the yield.

The stability of the yield means how large the fluctuations in the different yields are. For a perfect measurement, every fit would describe the number of entries perfectly and would therefore be the same. Thus, naively we would expect the ratio to be 1. Of course, when really doing the experiment, this turns out not to be true. Large fluctuations in the ratio point to a high systematic error, because clearly our obtained yield depends highly on the method we chose to determine it. The systematic error has to be less than the maximum spread, and it is most common to use half the spread as an estimate for the systematic error of the yield.

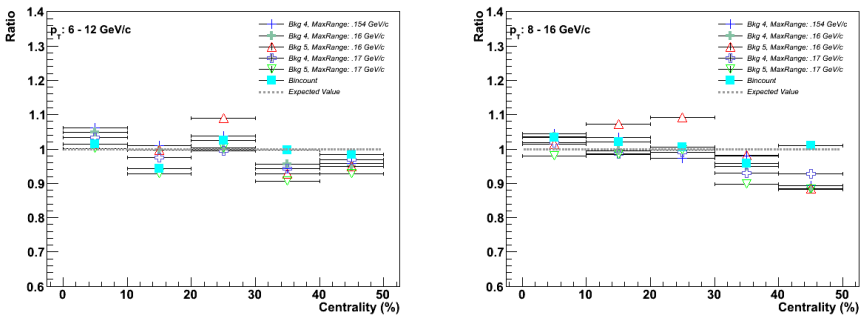

Figure 15: The ratio of the raw yield for the two different p_T-bins.

In figure 15 we see the ratio plotted for the two p_{T} bins. The actual values are in Table 1 and 2.

Centrality (%)	**Maximum spread (%)**	**Systematic error (%)**
0 - 10	6.1	3.1
10 - 20	8.3	4.1
20 - 30	9.7	4.9
30 - 40	9.4	4.7
40 - 50	8.6	4.3

Table 1: Systematic error for p_{T} bin between 6 and 12 GeV/c.

Centrality (%)	**Maximum spread (%)**	**Systematic error (%)**
0 - 10	6.4	3.2
10 - 20	8.8	4.4
20 - 30	12.2	6.1
30 - 40	10.3	5.1
40 - 50	11.9	5.9

Table 2: Systematic error for p_{T} bin between 8 and 16 GeV/c.

5.2 Particle Identification at high p_{T}

In section 5.1 we discussed the systematic error due to acquiring the yield. However, as we discussed before, we also have to identify the particles as being the pions and kaons we are looking for. This of course also happens within a given probability and therefore also gives rise to a systematic uncertainty. It is determined in a way similar to what we have seen when determining the systematic error of the yield. We now compare the yield of the fit without PID to the yield of the fit with PID. The ratio is

$$\text{Ratio } = \frac{\text{Yield from fit with PID}}{\text{Yield without PID}}. \tag{15}$$

We have to throw away a certain number of measured D mesons, because otherwise too much background is also counted as signal. The percentage of entries thrown away can be calculated from the number of sigma's used in both detectors. They are both applied twice, so the portion left is (the area under the peak within $\sigma_{TPC})^2$ * (the area under the peak within $\sigma_{TOF})^2$. For the very central collisions (0-20%), $\sigma_{TPC} = 2$ and $\sigma_{TOF} = 3$, so the expected ratio ≈ 0.9. For more peripheral collisions we have $\sigma_{TPC} = 3$ and $\sigma_{TOF} = 3$, so the expected ratio ≈ 0.98. Now, the difference between the actual ratio and the expected value is our systematic error due to PID.

The first results that were attained can be found in figure 16. Now, the systematic error is half the difference between the expected value and the measured value. It is clear that the systematic error due to PID in this plot is enormous, sometimes as large as 30%. This would make our results essentially useless,

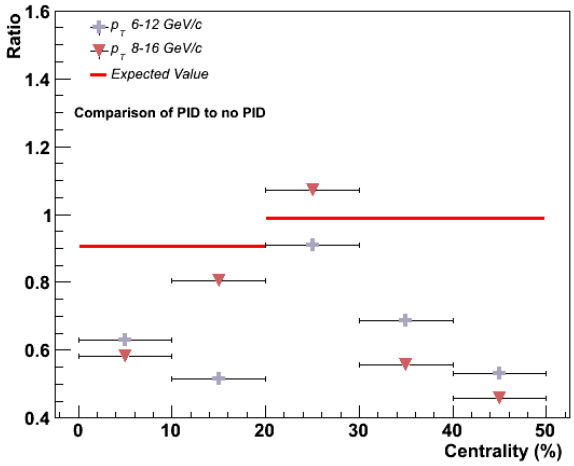

Figure 16: The ratio of the raw yield for PID compared to no PID for the two different p_{T} bins with specific ionisation energy loss cut turned on, leading to very high systematic errors.

because it would be nearly impossible to get significant results. The reason for this lies in the particle identification in the TPC at higher p_{T}.

As we can see in figure 17 the energy loss $\frac{dE}{dx}$, which is one of the PID-cuts that is applied, works only for the low p_{T} regions. First, the energy loss declines with increasing p_{T}, but this reverses for higher p_{T}. This process is called 'relativistic rise'. The parametrization being off makes our cuts useless or even harmful. Therefore, it is turned off for p_{T} higher than 4 GeV/c. Since in this paper we are looking at transverse momenta over 6 GeV/c, it is no longer of any meaning here.

If we now recalculate the ratios, we get figure 18. We see that except for the centrality bin 30-40%, everything is now within 1σ of the expected value.

Centrality (%)	**Systematic error (%)**
0 - 10	6
10 - 20	2
20 - 30	4
30 - 40	11
40 - 50	7

Table 3: Systematic error due to PID for p_{T} bin between 6 and 12 GeV/c.

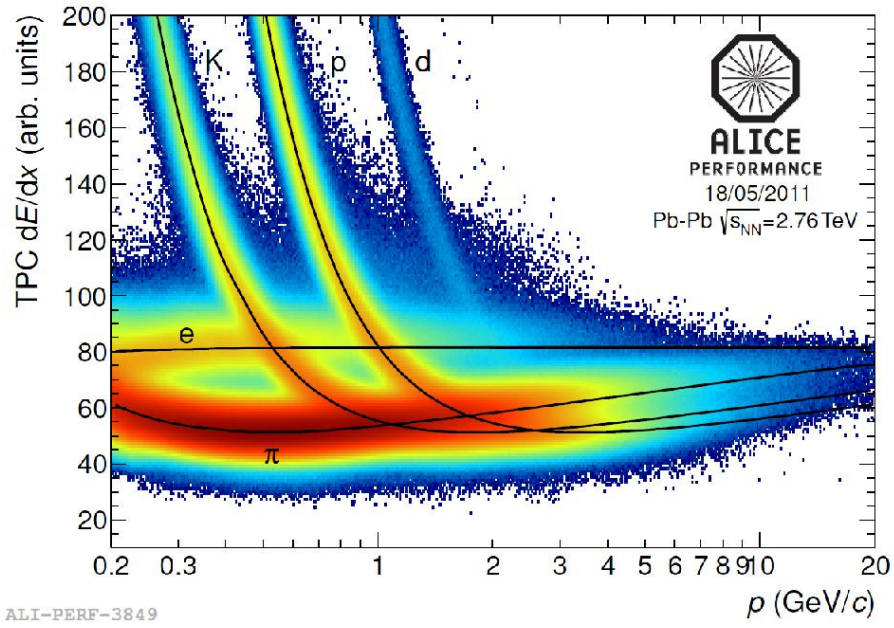

Figure 17: Specific ionisation energy loss (dE/dx) in the TPC for Pb-Pb collisions at $\sqrt{s_{NN}} = 2.76$ TeV.

Centrality (%)	**Systematic error (%)**
0 - 10	1
10 - 20	1
20 - 30	1
30 - 40	14
40 - 50	2

Table 4: Systematic error due to PID for p_{T} bin between 8 and 16 GeV/c.

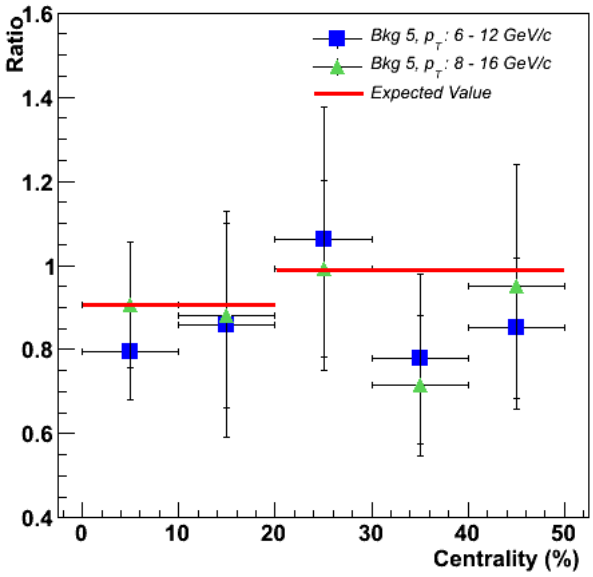

Figure 18: Final ratio of the raw yield for PID compared to no PID for the two different p_{T}-bins, with specific ionisation energy loss cut turned off.

6 Efficiency

We want to calculate the nuclear modification factor of the prompt D mesons, and not the ones feed down from B meson decays. For this, we have to know the efficiency of our detector for the prompt D mesons. We get this efficiency from our Monte Carlo sample, which is described in section 3.2. From this, we get a multidimensional histogram, in which all of the 16 steps the reconstruction procedure includes can be checked against each other. From this 256-dimensional histogram we check for each step how many of the generated D mesons from charm would be counted as a D meson by the detector. From this we get a ratio, the efficiency. It can be found for different steps and is plotted in the figures 19 and 20.

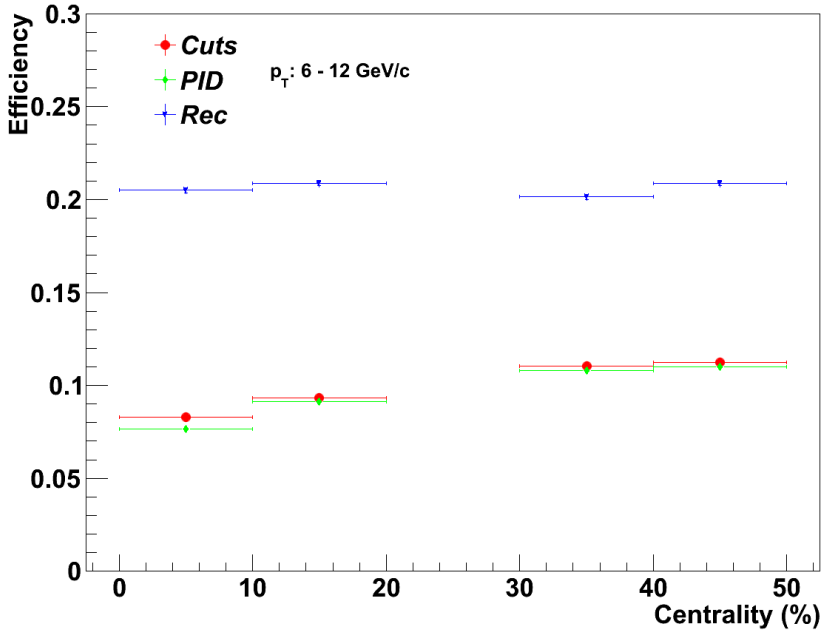

Figure 19: The efficiency for 6< p_{T} <12 GeV/c.

The most important data points are the ones called PID. This is the final efficiency, which is the number of generated D mesons that are actually detected after all cuts including PID have been applied. We notice that the efficiency varies, but generally increases with centrality and p_{T} and is approximately 10%. These values are consistent with other studies [6]. Once we have corrected for the detector efficiency, we can really calculate the number of D mesons produced in the collision, and from there the nuclear modification factor R_{AA}.

In figure 19, the efficiency for the 20-30% centrality bin is missing, because the most important thing was calculating the R_{AA} for p_{T} between 8 and 16 GeV/c, which will be explained in the following section.

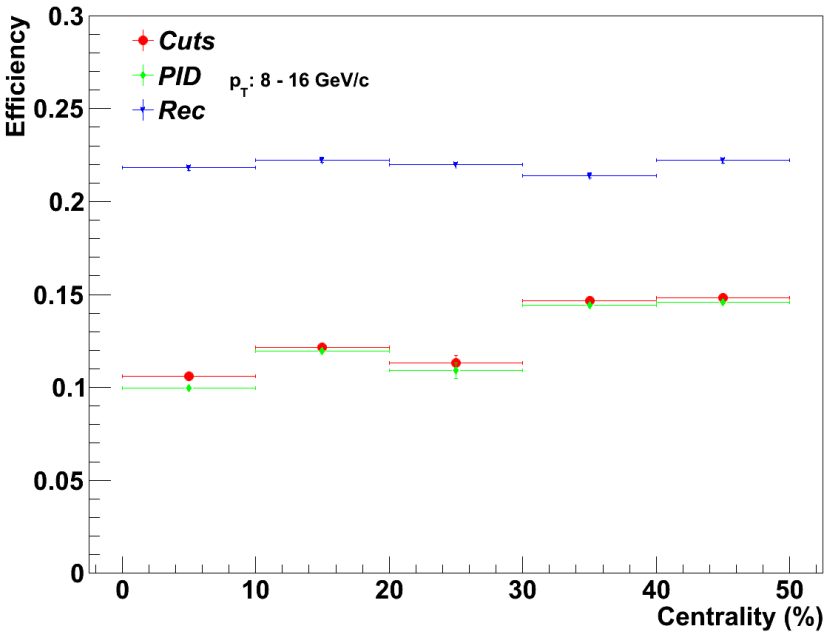

Figure 20: The efficiency for 8< p_{T} <16 GeV/c.

7 Nuclear modification factor

Finally, we come to the goal of this analysis. We are now able to determine the nuclear modification factor R_{AA}, as introduced in equation 1. It is plotted in figure 21.

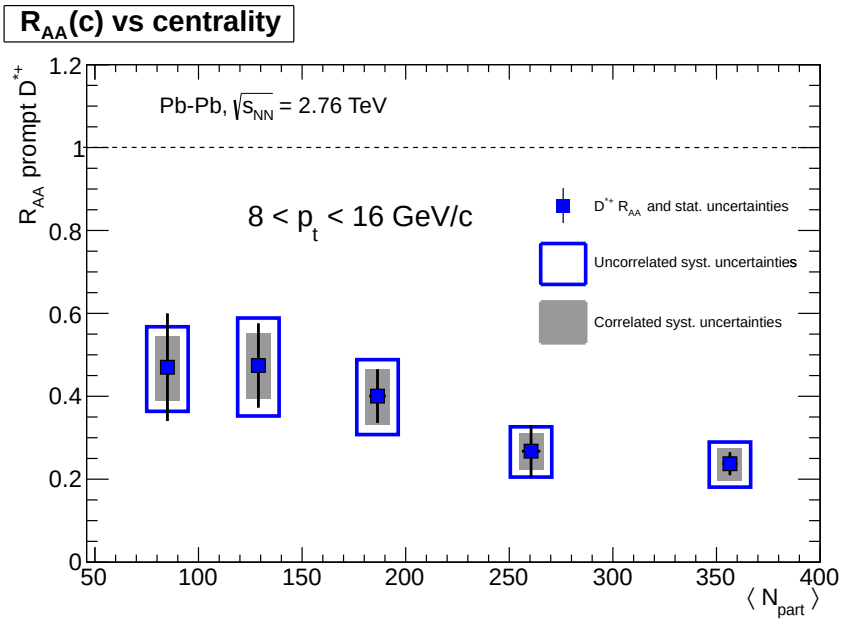

Figure 21: The nuclear modification factor versus the mean number of nucleons-participants of the collision for prompt D^{*+} for p_T between 8 - 16 GeV/c. A higher $< N_{\text{part}} >$ corresponds to a lower centrality.

In the figure we see the R_{AA} versus the mean number nucleons-participants of the collisions, $< N_{\text{part}} >$. In central collisions, more nucleons participate, so it is also a measure of the centrality. A higher $< N_{\text{part}} >$ thus corresponds to more central collisions. From this it follows that, as expected, for the most peripheral collisions, the suppression is the strongest, up to a factor 5. For more peripheral collisions, the R_{AA} steadily increases to approximately 0.5 for centrality 40-50% [7, 8].

This analysis was done for p_T between 8 and 16 GeV/c first, because it resembles most closely another experiment done in the CMS detector. In this experiment the R_{AA} was calculated for non prompt J/Ψ mesons. But this comparison is outside the scope of this thesis.

8 Conclusions and outlook

In this thesis we have seen we can calculate the systematic uncertainty for yield extraction and particle identification by determining the yield with different methods and then determining the ratio. The systematic uncertainty for yield extraction was calculated to be 3-6%, increasing for higher centrality and p_{T}. The systematics on the PID were determined to be 1-6%, except for one centrality bin in which the uncertainty was much larger. Also, the reconstruction efficiency was determined from a Monte Carlo sample. Increasing with p_{T} and centrality, values of approximately 10% were found. From this, it was possible to calculate the nuclear modification factor, which was 0.2 for the most central collisions and also increased with centrality, as expected.

One might conclude from this paper that now we have calculated the nuclear modification factor, we are done. This is not the case. We are still working with relatively high systematic uncertainties, specifically with centrality 30-40% for PID. At this moment in time, it is not clear why this is. More data analysis might lead to more exact results, which would lead to a better insight in the properties of the QGP. Also, it would be interesting to see the centrality dependence of the R_{AA} for different p_{T} bins. But this is outside the scope of this thesis.

References

[1] Loïc Manceau, "B and D hadron inclusive cross-section measurement with the ALICE muon spectrometer at LHC." http://lmanceau.web.cern.ch/lmanceau/English/Topic/Topic.html

[2] Jasper van der Maarel "D^{*+} analysis in proton-proton at $\sqrt{s} = 7$ TeV at ALICE," Bachelor thesis, Utrecht University (2011).

[3] Piotr Kukla, "D^{*+} analysis in proton-proton at $\sqrt{s} = 2.76$ TeV using the ALICE detector at CERN," Master thesis, Utrecht University (2011).

[4] [ALICE Collaboration] *et al.*, J. Phys. G: Nucl. Part. Phys. 30 (2004) 1517

[5] K. Nakamura et al. [Particle Data Group], J. Phys. G37 (2010) 075021, and 2011 partial update for the 2012 edition.

[6] B. Abelev *et al.* [ALICE Collaboration], "Measurement of charm production at central rapidity in proton-proton collisions at $\sqrt{s} = 2.76$ TeV," JHEP **1207** (2012) 191.

[7] A. Grelli [ALICE Collaboration], "D meson nuclear modification factors in Pb-Pb collisions at $\sqrt{s_{NN}} = 2.76$ TeV with the ALICE detector," arXiv:1210.7332, submitted to Nuclear Physics A.

[8] B. Abelev *et al.* [ALICE Collaboration], "Suppression of high transverse momentum D mesons in central Pb-Pb collisions at $\sqrt{s_{NN}} = 2.76$ TeV," JHEP **1209** (2012) 112